Noise spectra of ac-driven quantum dots: Floquet master-equation approach

B. H. Wu[1,2,*] and C. Timm[3,†]

[1]*Max Planck Institute for the Physics of Complex Systems, Nöthnitzer Strasse 38, 01087 Dresden, Germany*

[2]*State Key Laboratory of Functional Materials for Informatics, Shanghai Institute of Microsystem and Information Technology, 865 Changning Road, Shanghai 200050, China*

[3]*Institute for Theoretical Physics, Technische Universität Dresden, 01062 Dresden, Germany*

We study the transport properties of a quantum dot driven by either a rotating magnetic field or an ac gate voltage using the Floquet master-equation approach. Both types of ac driving lead to photon-assisted tunneling where quantized amounts of energy are exchanged with the driving field. It is found that the differential-conductance peak due to photon-assisted tunneling does not survive in the Coulomb-blockade regime when the dot is driven by a rotating magnetic field. Furthermore, we employ a generalized MacDonald formula to calculate the time-averaged noise spectra of ac-driven quantum dots. Besides the peak at zero frequency, the noise spectra show additional peaks or dips in the presence of an ac field. For the case of an applied ac gate voltage, the peak or dip position is fixed at the driving frequency whereas the position changes with increasing amplitude for the case of a rotating magnetic field. Additional features appear in the noise spectra if a dc magnetic field is applied in addition to a rotating field. In all cases, the peak or dip positions can be understood from the energy differences of two available Floquet channels.

I. INTRODUCTION

Quantum conductors based on single molecules or semiconductor quantum dots are promising building blocks for future electronics and model systems for the study of fundamental quantum phenomena.[1] However, much information on quantum conductors is beyond the reach of measurements of the current or conductance alone. Instead, the understanding of the transport properties calls for a study of the full counting statistics.[2–11] In the past decade, valuable information on microscopic details of the charge transport has been obtained from measurements of the current fluctuations or current noise.[12] Previous studies have shown that one can extract parameters such as the average backscattered charge,[13] the intrinsic time scales,[14,15] and the asymmetry of the dot-lead coupling[16,17] from current-noise measurements. Most studies of the current noise have focused on the zero-frequency noise power $S(0)$.[18–20] The zero-frequency noise reflects the average properties of the tunneling. Since the finite-frequency current noise $S(\omega)$ is a measure of the correlations between tunneling events with their time difference conjugate to the frequency ω,[21] it is interesting to go beyond the zero-frequency limit. Aguado and Brandes[14] have demonstrated that the noise spectra can show dip structures at the splitting energy of an open quantum two-level system, with their width controlled by its dissipative dynamics. In many works, the MacDonald formula[22] has been used to study the current-noise spectra.[23–25]

Effective *in situ* manipulation of quantum conductors is a key step for further development. Using a time-dependent field to manipulate the dynamics of quantum dots promises to be advantageous in situations ranging from photon-assisted inelastic tunneling[26] to quantum pumping.[27] When the conductor is driven by an ac field, one expects novel features due to the interplay of intrinsic oscillation frequencies and the external driving frequency. Several recent studies[28,29] indicate that key information is hidden in the noise spectra of the ac-driven transport. For instance, Barrett and Stace[28] have proposed to extract the characteristic time scales such as the inverse dephasing and relaxation rates of a solid-state charge qubit coupled to a microwave field from the noise spectrum. Wabnig *et al.*[29] have proposed to estimate the coherence time of the spin in a quantum dot by measuring its noise spectra under an ac magnetic field. These results are obtained based on the rotating-wave approximation and usually in the limit of infinite on-site Coulomb interaction.

For periodically driven systems, an appropriate theoretical tool to go beyond the rotating-wave approximation is the Floquet theorem.[30,31] Various attempts have been made by generalizing the existing steady-state transport approaches such as the scattering matrix[32–34] and nonequilibrium Green's functions[35–37] with the help of the Floquet theorem. However, these methods are not adequate to fully take the Coulomb blockade in quantum dots into account, which dominates the transport properties of small-size quantum conductors. The quantum master equation[38] in its various manifestations[39,40] is able to give a good account of the Coulomb blockade in the weak-tunneling limit. This method has previously been generalized using the Floquet theorem to study the current and the zero-frequency noise power in an ac-driven conductor.[38,41–45]

In the present study, we employ the Floquet master equation in the Fock space of an ac-driven quantum dot to study the transport properties such as the differential conductance and the full noise spectrum in the sequential-tunneling limit. As the ac field we consider a rotating magnetic field as well as an ac gate voltage for comparison. We employ a generalized MacDonald formula for the time-averaged noise spectra in the presence of a periodic ac field. An equivalent form of the generalized MacDonald formula has been given by Clerk and Girvin[46] without derivation. For completeness, we present a derivation in the Appendix. Note that the authors

are concerned with a different case, namely, an ac *bias* voltage and do not employ the Floquet formalism.

Our paper is organized as follows. In Sec. II, a Floquet master-equation formalism is presented to study the transport properties of ac-driven quantum dots. Expressions for the noise spectra are derived based on the full counting statistics and the generalized MacDonald formula. In Sec. III, the transport properties of the ac-driven quantum dot are studied. The ac field is either a rotating magnetic field or an oscillating on-site energy due to a periodic gate voltage. The characteristic features in the transport properties are presented and discussed. In Sec. IV, a brief summary is given.

II. FORMALISM

A. Model

In this paper, we study the transport properties of a single-level quantum dot driven by an ac field. The quantum dot is coupled to the left (L) and right (R) electron leads. The leads are assumed to be ideal and free of interactions. The Hamiltonian of the model system can be written as

$$H(t) = H_L + H_R + H_{\rm dot}(t) + H_T \equiv H_0 + H_T, \quad (1)$$

where $H_{\rm dot}$ is the Hamiltonian of the isolated quantum dot, which contains the effects of the ac field and the Coulomb interaction, $H_l = \Sigma_{\mathbf{k}\sigma} \epsilon_{l\mathbf{k}\sigma} c_{l\mathbf{k}\sigma}^\dagger c_{l\mathbf{k}\sigma}$ represents the Hamiltonian of lead $l = L, R$, where $c_{l\mathbf{k}\sigma}$ ($c_{l\mathbf{k}\sigma}^\dagger$) annihilates (creates) an electron with spin σ, crystal momentum $\mathbf{k}$, and energy $\epsilon_{l\mathbf{k}\sigma}$ in lead l, and $H_T = \Sigma_{l\mathbf{k}\sigma} V_{l\mathbf{k}\sigma} c_{l\mathbf{k}\sigma}^\dagger d_\sigma + {\rm H.c.}$ describes the coupling between the quantum dot and the leads, where $d_\sigma^\dagger$ (d_σ) is the spin-σ electron creation (annihilation) operator in the quantum dot. We note that we do not assume an infinite Coulomb-interaction strength $U \to \infty$, in contrast to previous studies.[44] Instead, finite Coulomb interaction will be included by taking the doubly occupied state into account.

In the following, we focus on the limit of weak dot-lead coupling and investigate the transport properties of the quantum dot using the Floquet master-equation method. For a small quantum dot, for which the Coulomb interaction can dominate the transport behavior, the treatment of the Coulomb interaction must go beyond the mean-field level. To this end, it is convenient to rewrite the dot Hamiltonian in the electron-number basis of the Fock space.[47,48] In this description, the quantum dot can either be in the empty state $|0\rangle$, the singly occupied state $|\sigma\rangle$ with spin $\sigma = \uparrow$ or $\downarrow$, or the doubly occupied state $|\uparrow\downarrow\rangle$. In the following, we denote the states in the Fock space by Latin letters, $|a\rangle = |0\rangle, |\uparrow\rangle, |\downarrow\rangle, |\uparrow\downarrow\rangle$. Using this orthonormal basis, the dot-lead coupling can be described naturally with the help of Hubbard operators,

$$X_{ab} = |a\rangle\langle b|, \quad (2)$$

which describes the transition of the quantum dot from state $|b\rangle$ to state $|a\rangle$. The second-quantized dot-electron creation operator can thus be rewritten in terms of the Hubbard operators as

$$d_\sigma^\dagger = |\sigma\rangle\langle 0| + \eta_\sigma |\uparrow\downarrow\rangle\langle\bar\sigma|, \quad (3)$$

where $\bar\sigma$ represents the opposite spin of σ and the factor $\eta_\sigma = \pm 1$ for $\sigma = \uparrow, \downarrow$, respectively, is due to the anticommutation relation of the fermions. In terms of these Hubbard operators, the Hamiltonian for the dot-lead coupling and the isolated dot can be rewritten as

$$H_{\rm dot} = \sum_{ab} H_{ab}^D |a\rangle\langle b|, \quad (4)$$

$$H_T = \sum_{ab,l\mathbf{k}\sigma} V_{l\mathbf{k}\sigma}^{ab} c_{l\mathbf{k}\sigma}^\dagger X_{ab} + {\rm H.c.}, \quad (5)$$

respectively. Here, we have made the coupling strength $V_{l\mathbf{k}\sigma}^{ab}$ depend on the occupancy of the initial and final states of the transition in the quantum dot. The explicit form of the dot Hamiltonian depends on the details of the device geometry and the external ac-driving field. It will be specified in the following sections.

B. Floquet quantum-master-equation approach

1. Floquet states

Due to the presence of a time-periodic external field, the dynamics of the quantum dot is governed by a Hamiltonian that is periodic in time with the frequency $\Omega = 2\pi/\mathcal{T}$, i.e., $H_{\rm dot}(t) = H_{\rm dot}(t+\mathcal{T})$, where $\mathcal{T}$ denotes the period. The solution of the time-periodic Hamiltonian can be simplified by the Floquet theorem,[30,31] which states that the solution of the Schrödinger equation for the dot Hamiltonian can be obtained from (we set $\hbar = |e| = k_B = 1$ in the following)

$$\left[H_{\rm dot}(t) - i\frac{\partial}{\partial t} \right] |\alpha(t)\rangle = \varepsilon_\alpha |\alpha(t)\rangle, \quad (6)$$

where ε_α is the time-independent Floquet quasienergy and $|\alpha(t)\rangle$ is the corresponding Floquet state, which has the same period $\mathcal{T}$, $|\alpha(t)\rangle = |\alpha(t+\mathcal{T})\rangle$. Here, Greek letters are used to denote the Floquet states. Further simplification is possible by decomposing the Floquet states into a Fourier series,

$$|\alpha(t)\rangle = \sum_k e^{-ik\Omega t} |\alpha_k\rangle \quad (7)$$

with the reverse transformation

$$|\alpha_k\rangle = \frac{1}{\mathcal{T}} \int_0^\mathcal{T} dt\, e^{ik\Omega t} |\alpha(t)\rangle \quad (8)$$

and analogously for $H_{\rm dot}(t)$. The Fourier transform of Eq. (6) then reads

$$\sum_{k'} H_{{\rm dot},k-k'} |\alpha_{k'}\rangle - k\Omega |\alpha_k\rangle = \varepsilon_\alpha |\alpha_k\rangle. \quad (9)$$

The quasienergy ε_α can evidently be restricted to the first Brillouin zone $[0,\Omega)$ of the Floquet space while the Floquet index k can assume any integer value. Equivalently, we can view $\varepsilon_\alpha + k\Omega$ as the quasienergy in the extended zone scheme.

We also introduce the Hubbard operator in the Floquet states to describe the transition between the Floquet states as

$X_{\alpha\beta}(t) = |\alpha(t)\rangle\langle\beta(t)|$. For the time-dependent transport, it is more convenient to work with these Floquet states. This is most advantageous in transformations of the following form, which we will use in the derivation below,

$$\widetilde{X}_{\alpha\beta}(t',t) = U_0^\dagger(t',t)X_{\alpha\beta}(t')U_0(t',t) = e^{i(\varepsilon_\beta-\varepsilon_\alpha)(t-t')}X_{\alpha\beta}(t), \tag{10}$$

where

$$U_0(t',t) = T_c \exp\left(-i\int_t^{t'} dt''[H_L + H_R + H_{\mathrm{dot}}(t'')]\right) \tag{11}$$

denotes the time-evolution operator due to the Hamiltonian in the absence of tunneling. Here, T_c is the time-ordering operator and the dot Hamiltonian is explicitly time dependent.

2. Floquet quantum master equation with counting fields

For a quantum dot coupled to external leads, the exact quantum master equation can be written in the interaction picture as[38,39]

$$\frac{d}{dt}\rho_I(t) = -i[H_{T,I}(t),\rho_I(t_0)] - \int_{t_0}^t dt'[H_{T,I}(t),[H_{T,I}(t'),\rho_I(t')]], \tag{12}$$

where $A_I(t) = U_0^\dagger(t,t_0)A(t)U_0(t,t_0)$ denotes an operator in the interaction picture and $\rho(t)$ is the density matrix in the Fock space of the full system.

A complete description of the electronic transport through the quantum dot is provided by the full counting statistics. Properties such as the noise spectrum are determined by the counting statistics of the electrons arriving at and departing from the leads. All information on the counting statistics is contained in the moment-generating function $\phi(\chi_L,\chi_R) = \langle\exp(i\chi_L N_L + i\chi_R N_R)\rangle$. Here, χ_l represents the counting field in the lead l, which counts how many electrons have tunneled into or out of the lead. $N_l = \sum_{\mathbf{k}\sigma} c_{l\mathbf{k}\sigma}^\dagger c_{l\mathbf{k}\sigma}$ is the electron-number operator in lead l. We introduce the operator

$$\mathcal{F}(\chi_L,\chi_R,t) = \mathrm{Tr}_{\mathrm{leads}}\, e^{i\chi_L N_L + i\chi_R N_R}\rho(t). \tag{13}$$

In this we follow Kaiser and Kohler,[44] except that we introduce two counting fields. In the limit of $\chi_L \to 0$ and $\chi_R \to 0$, $\mathcal{F}$ becomes the reduced density matrix of the quantum dot, $\rho_{\mathrm{dot}} = \mathrm{Tr}_{\mathrm{leads}}\,\rho$. Moreover, the moment-generating function $\phi(\chi_L,\chi_R,t)$ can be obtained by tracing out the dot degrees of freedom, $\phi = \mathrm{Tr}_{\mathrm{dot}}\,\mathcal{F}$. We decompose $\mathcal{F}$ into a Taylor series,

$$\mathcal{F} = \sum_{m=0}^\infty \sum_{n=0}^\infty \frac{(i\chi_L)^m(i\chi_R)^n}{m!n!}\mathcal{F}^{m,n}, \tag{14}$$

where the coefficients

$$\mathcal{F}^{m,n} = \frac{\partial^{m+n}}{\partial^m(i\chi_L)\partial^n(i\chi_R)}\mathcal{F}\bigg|_{\chi_L,\chi_R\to 0} = \mathrm{Tr}_{\mathrm{leads}}\, N_L^m N_R^n\rho \tag{15}$$

provide a direct access to the moments $\langle N_L^m N_R^n\rangle = \mathrm{Tr}_{\mathrm{dot}}\,\mathcal{F}^{m,n}$. In particular, we obtain the reduced density matrix of the quantum dot, $\rho_{\mathrm{dot}} = \mathcal{F}^{0,0}$.

To find the solutions for $\mathcal{F}$, we first transform the equation of motion for the density matrix in the interaction picture, Eq. (12), back to the Schrödinger picture,

$$\frac{d\rho(t)}{dt} + i[H_0(t),\rho(t)] = -i[H_T,U_0^\dagger(t_0,t)\rho(t_0)U_0(t_0,t)]$$
$$- \int_{t_0}^t dt'[H_T,U_0^\dagger(t',t)$$
$$\times[H_T,\rho(t')]U_0(t',t)]. \tag{16}$$

Then, we multiply by $e^{i\chi_L N_L + i\chi_R N_R}$ from the left and take the trace over the lead degrees of freedom to obtain

$$\frac{d\mathcal{F}(\chi_L,\chi_R,t)}{dt} + i[H_{\mathrm{dot}}(t),\mathcal{F}(\chi_L,\chi_R,t)]$$
$$= -i\,\mathrm{Tr}_{\mathrm{leads}}\, e^{i\chi_L N_L + i\chi_R N_R}[H_T,U_0^\dagger(t_0,t)\rho(t_0)U_0(t_0,t)]$$
$$- \int_{t_0}^t dt'\,\mathrm{Tr}_{\mathrm{leads}}\, e^{i\chi_L N_L + i\chi_R N_R}[H_T,U_0^\dagger(t',t)$$
$$\times[H_T,\rho(t')]U_0(t',t)], \tag{17}$$

which is still exact.

We now assume that the full density operator is of product form at the initial time t_0, $\rho(t_0) = \rho_{\mathrm{dot}}(t_0) \otimes \rho_{\mathrm{leads}}^0$, where ρ_{leads}^0 describes the leads in separate thermal equilibrium. This assumption is reasonable since we are not interested in transient effects coming from the initial state. Such effects have been studied by Flindt et al.[49] The first term on the right-hand side of Eq. (17) then vanishes. Furthermore, we make the sequential-tunneling approximation appropriate for weak tunneling, i.e., we treat the tunneling perturbatively to second order in H_T. Since two powers of H_T are already explicit in the second term on the right-hand side of Eq. (17), we can express $\rho(t')$ in terms of the unperturbed time evolution, $\rho(t') \approx U_0^\dagger(t,t')\rho(t)U_0(t,t')$. This makes the master equation local in time, i.e., Markovian. For details, see, e.g., Ref. 39. We thus do not include non-Markovian effects as studied by Flindt et al.[49] This is valid if the relaxation time in the leads is short compared to the typical time scales of the dot, which in our case include the period of the ac field. Since relaxation times in metallic leads are on the order of femtoseconds, this is easily satisfied.

Finally, we send $t_0 \to -\infty$ and obtain

$$\frac{d\mathcal{F}(\chi_L,\chi_R,t)}{dt} + i[H_{\mathrm{dot}}(t),\mathcal{F}(\chi_L,\chi_R,t)]$$
$$= -\int_0^\infty d\tau\,\mathrm{Tr}_{\mathrm{leads}}\, e^{i\chi_L N_L + i\chi_R N_R}[H_T,[\widetilde{H}_T(t-\tau,t),\rho(t)]], \tag{18}$$

where $\widetilde{H}_T(t',t) = U_0^\dagger(t',t)H_T U_0(t',t)$.

To obtain the Floquet master equation, we write Eq. (18) in the basis of Floquet states $|\alpha(t)\rangle$ and $|\beta(t)\rangle$. By making use of the relation Eq. (10) and tracing out the lead degrees of freedom, we arrive at the equation of motion for $\mathcal{F}$,

$$\frac{d}{dt}\mathcal{F}_{\alpha\beta}(\chi_L,\chi_R,t) = \{[\mathcal{L} + (e^{i\chi_L}-1)\mathcal{J}_{L+} + (e^{-i\chi_L}-1)\mathcal{J}_{L-} + (e^{i\chi_R}-1)\mathcal{J}_{R+} + (e^{-i\chi_R}-1)\mathcal{J}_{R-}]\mathcal{F}(\chi_L,\chi_R,t)\}_{\alpha\beta}, \quad (19)$$

where the superoperators are given by

$$(\mathcal{L}\mathcal{F})_{\alpha\beta} = -i(\varepsilon_\alpha - \varepsilon_\beta)\mathcal{F}_{\alpha\beta} + \frac{1}{2\pi}\int_0^\infty d\tau \int d\varepsilon \sum_{ab;mn}\sum_{\gamma\delta}\sum_{l=L,R;\sigma}\left\{-[f_l(\varepsilon)e^{i\varepsilon\tau}\mathrm{T}^{l\sigma}_{ab;mn}(\varepsilon) + \bar{f}_l(\varepsilon)e^{-i\varepsilon\tau}\mathrm{T}^{l\sigma}_{mn;ab}]\right.$$

$$\times e^{i(\varepsilon_\delta-\varepsilon_\gamma)\tau}\langle\alpha(t)|a\rangle\langle b|\gamma(t)\rangle\langle\gamma(t-\tau)|m\rangle\langle n|\delta(t-\tau)\rangle\mathcal{F}_{\delta\beta}(\chi_L,\chi_R,t)$$

$$+ [\bar{f}_l(\varepsilon)e^{i\varepsilon\tau}\mathrm{T}^{l\sigma}_{ab;mn}(\varepsilon) + f_l(\varepsilon)e^{-i\varepsilon\tau}\mathrm{T}^{l\sigma}_{mn;ab}]e^{i(\varepsilon_\beta-\varepsilon_\delta)\tau}\langle\alpha(t)|a\rangle\langle b|\gamma(t)\rangle\mathcal{F}_{\gamma\delta}(\chi_L,\chi_R,t)\langle\delta(t-\tau)|m\rangle\langle n|\beta(t-\tau)\rangle$$

$$+ [\bar{f}_l(\varepsilon)e^{-i\varepsilon\tau}\mathrm{T}^{l\sigma}_{ab;mn}(\varepsilon) + f_l(\varepsilon)e^{i\varepsilon\tau}\mathrm{T}^{l\sigma}_{mn;ab}]e^{i(\varepsilon_\gamma-\varepsilon_\alpha)\tau}\langle\alpha(t-\tau)|a\rangle\langle b|\gamma(t-\tau)\rangle\mathcal{F}_{\gamma\delta}(\chi_L,\chi_R,t)\langle\delta(t)|m\rangle\langle n|\beta(t)\rangle$$

$$\left. - [\bar{f}_l(\varepsilon)e^{i\varepsilon\tau}\mathrm{T}^{l\sigma}_{mn;ab}(\varepsilon) + f_l(\varepsilon)e^{-i\varepsilon\tau}\mathrm{T}^{l\sigma}_{ab;mn}]e^{i(\varepsilon_\delta-\varepsilon_\gamma)\tau}\mathcal{F}_{\alpha\gamma}(\chi_L,\chi_R,t)\langle\gamma(t-\tau)|a\rangle\langle b|\delta(t-\tau)\rangle\langle\delta(t)|m\rangle\langle n|\beta(t)\rangle\right\}, \quad (20)$$

$$(\mathcal{J}_{l+}\mathcal{F})_{\alpha\beta} = \frac{1}{2\pi}\int_0^\infty d\tau \int d\varepsilon \sum_{ab;mn}\sum_{\gamma\delta}\sum_\sigma \bar{f}_l(\varepsilon)\Gamma^{l\sigma}_{ab;mn}[e^{i\varepsilon\tau}e^{i(\varepsilon_\beta-\varepsilon_\delta)\tau}\langle\alpha(t)|a\rangle\langle b|\gamma(t)\rangle\mathcal{F}_{\gamma\delta}(\chi_L,\chi_R,t)\langle\delta(t-\tau)|m\rangle\langle n|\beta(t-\tau)\rangle$$

$$+ e^{-i\varepsilon\tau}e^{i(\varepsilon_\gamma-\varepsilon_\alpha)\tau}\langle\alpha(t-\tau)|a\rangle\langle b|\gamma(t-\tau)\rangle\mathcal{F}_{\gamma\delta}(\chi_L,\chi_R,t)\langle\delta(t)|m\rangle\langle n|\beta(t)\rangle], \quad (21)$$

$$(\mathcal{J}_{l-}\mathcal{F})_{\alpha\beta} = \frac{1}{2\pi}\int_0^\infty d\tau \int d\varepsilon \sum_{ab;mn}\sum_{\gamma\delta}\sum_\sigma f_l(\varepsilon)\Gamma^{l\sigma}_{mn;ab}[e^{-i\varepsilon\tau}e^{i(\varepsilon_\beta-\varepsilon_\delta)\tau}\langle\alpha(t)|a\rangle\langle b|\gamma(t)\rangle\mathcal{F}_{\gamma\delta}(\chi_L,\chi_R,t)\langle\delta(t-\tau)|m\rangle\langle n|\beta(t-\tau)\rangle$$

$$+ e^{i\varepsilon\tau}e^{i(\varepsilon_\gamma-\varepsilon_\alpha)\tau}\langle\alpha(t-\tau)|a\rangle\langle b|\gamma(t-\tau)\rangle\mathcal{F}_{\gamma\delta}(\chi_L,\chi_R,t)\langle\delta(t)|m\rangle\langle n|\beta(t)\rangle]. \quad (22)$$

Here, we have defined the tunneling rate $\Gamma^{l\sigma}_{mn;ab}(\epsilon) = 2\pi\rho_l(\epsilon)V^{ab}_{l,k,\sigma}V^{mn*}_{l,k,\sigma}$, where $\rho_l(\epsilon)$ is the density of states in lead l.

Inserting the Taylor expansion of $\mathcal{F}$ in Eq. (14) into its equation of motion [Eq. (19)], one obtains a hierarchy of equations for the expansion coefficients,

$$\frac{d}{dt}\mathcal{F}^{0,0} = \mathcal{L}\mathcal{F}^{0,0}, \quad (23)$$

$$\frac{d}{dt}\mathcal{F}^{1,0} = \mathcal{L}\mathcal{F}^{1,0} + (\mathcal{J}_{L+} - \mathcal{J}_{L-})\mathcal{F}^{0,0}, \quad (24)$$

$$\frac{d}{dt}\mathcal{F}^{0,1} = \mathcal{L}\mathcal{F}^{0,1} + (\mathcal{J}_{R+} - \mathcal{J}_{R-})\mathcal{F}^{0,0}, \quad (25)$$

$$\frac{d}{dt}\mathcal{F}^{2,0} = \mathcal{L}\mathcal{F}^{2,0} + 2(\mathcal{J}_{L+} - \mathcal{J}_{L-})\mathcal{F}^{1,0} + (\mathcal{J}_{L+} + \mathcal{J}_{L-})\mathcal{F}^{0,0}, \quad (26)$$

$$\frac{d}{dt}\mathcal{F}^{0,2} = \mathcal{L}\mathcal{F}^{0,2} + 2(\mathcal{J}_{R+} - \mathcal{J}_{R-})\mathcal{F}^{0,1} + (\mathcal{J}_{R+} + \mathcal{J}_{R-})\mathcal{F}^{0,0}, \quad (27)$$

$$\frac{d}{dt}\mathcal{F}^{1,1} = \mathcal{L}\mathcal{F}^{1,1} + (\mathcal{J}_{L+} - \mathcal{J}_{L-})\mathcal{F}^{0,1} + (\mathcal{J}_{R+} - \mathcal{J}_{R-})\mathcal{F}^{1,0}, \quad (28)$$

etc. As described above, these coefficients contain the full counting statistics. The charge current out of lead l is defined as the negative of the time derivative of the charge in lead l, $I_l(t) = edN_l/dt$. The final expression for the current out of the left lead is given by[44]

$$\langle I_L(t)\rangle = e\,\mathrm{Tr}_{\mathrm{dot}}\langle\dot{\mathcal{F}}^{1,0}\rangle = e\,\mathrm{Tr}_{\mathrm{dot}}(\mathcal{J}_{L+} - \mathcal{J}_{L-})\mathcal{F}^{0,0}. \quad (29)$$

The dc component of the current then gives the time average $\bar{I}$. In order to find $\mathcal{F}^{0,0}$, we have to solve a set of linear equations with the help of the normalization condition of probability $\mathrm{Tr}_{\mathrm{dot}}\,\mathcal{F}^{0,0}(t) = 1$.

3. Generalized MacDonald formula for time-averaged noise spectra

We are interested in the frequency-dependent current noise of the quantum dot driven by an ac field. The zero-frequency current noise for nonadiabatic driving has been investigated in Ref. 44 using the Floquet master-equation approach in the Coulomb-blockade regime. The symmetrized current-current correlation function is defined by

$$S_{ll'}(t,t') = \langle\hat{I}_l(t)\hat{I}_{l'}(t')\rangle + \langle\hat{I}_{l'}(t')\hat{I}_l(t)\rangle - 2\langle\hat{I}_l(t)\rangle\langle\hat{I}_{l'}(t')\rangle, \quad (30)$$

where $\hat{I}_l(t)$ represents the current operator at the time t from the lead l. The current-noise spectra are defined as the Fou-

rier transform of $S_{ll'}(t,t')$. Since our system is driven by an ac field, the current noise is a double-time function. However, the periodicity of our problem makes it possible to characterize the spectra by averaging over one driving period.

At finite frequencies, the total current $I(t)$ measured by a measurement device depends on both the particle and the displacement currents in the lead-dot-lead junction. If one expresses the displacement currents by the particle currents I_L and I_R, one obtains the Ramo-Shockley theorem,[12,50,51]

$$I(t) = aI_L(t) - bI_R(t). \tag{31}$$

Here the coefficients a and b, which satisfy $a+b=1$, are specified by the device geometry. It is straightforward to show that the total time-averaged noise spectrum is given by

$$\bar{S}(\omega) = a^2\bar{S}_{LL}(\omega) + b^2\bar{S}_{RR}(\omega) - ab[\bar{S}_{LR}(\omega) + \bar{S}_{RL}(\omega)], \tag{32}$$

where $\bar{S}_{ll'}(\omega)$ $(l,l'=L,R)$ represents the frequency-dependent time-averaged current correlation between I_l and $I_{l'}$,

$$\bar{S}_{ll'}(\omega) = \frac{1}{\mathcal{T}}\int_0^{\mathcal{T}} dt \int dt' e^{i\omega(t-t')} S_{ll'}(t,t'). \tag{33}$$

In this study, we used two counting fields to derive the noise spectra. An alternative approach is to calculate the charge fluctuation on the dot employing the quantum regression formula.[3,14,52,53] The two approaches are physically equivalent due to the charge conservation condition in the transport.

The formula for the zero-frequency noise has been presented in Ref. [44]. For the two-terminal device, it is adequate to find the time-averaged zero-frequency noise from the fluctuations of the current flowing out of a chosen lead, $\bar{S}(0) = \bar{S}_{ll}(0)$. The solution for $\bar{S}(0)$ resulting from the Floquet quantum master equation reads

$$\bar{S}(0) = \frac{2}{\mathcal{T}}\int_0^{\mathcal{T}} dt e^2 \, \text{Tr}_{\text{dot}}[2(\mathcal{J}_{l+} - \mathcal{J}_{l-})\mathcal{F}_{\perp}^{\delta_{lL},\delta_{lR}} + (\mathcal{J}_{l+} + \mathcal{J}_{l-})\mathcal{F}^{0,0}], \tag{34}$$

where the prefactor of 2 is inserted to make the noise formula consistent with Ref. [12]. For Poissonian noise, we then obtain $\bar{S}(0) = 2e\bar{I}$. δ_{ij} is the usual Kronecker symbol. Following Ref. [44], the new function $\mathcal{F}_{\perp}^{\delta_{lL},\delta_{lR}}$ in the noise expression is defined as

$$\mathcal{F}_{\perp}^{\delta_{lL},\delta_{lR}} = \mathcal{F}^{\delta_{lL},\delta_{lR}} - \mathcal{F}^{0,0} \, \text{Tr}_{\text{dot}}\{\mathcal{F}^{\delta_{lL},\delta_{lR}}\}, \tag{35}$$

and satisfies the equation of motion

$$\dot{\mathcal{F}}_{\perp}^{\delta_{lL},\delta_{lR}} = \mathcal{L}(t)\mathcal{F}_{\perp}^{\delta_{lL},\delta_{lR}} + \left(\mathcal{J}_{l+} - \mathcal{J}_{l-} - \frac{1}{e}\langle I_l(t)\rangle\right)\mathcal{F}^{0,0}. \tag{36}$$

An efficient method to find the noise spectrum is provided by the MacDonald formula,[22] which has been widely used in quantum transport.[21,23–25] The validity of this formula requires that the current correlation function $\langle I(t_1)I(t_2)\rangle$ is only a function of the time difference t_1-t_2 and that, therefore, the

transport is in the stationary regime. A direct application of the MacDonald formula to the present time-dependent transport problem is thus not possible. However, in the present study the driving field is time periodic. The discrete temporal translation symmetry $H(t+\mathcal{T})=H(t)$ makes it possible to generalize the MacDonald formula for the noise spectra time averaged over one period as

$$\frac{\bar{S}_{ll'}(\omega)}{\omega} = \frac{2e^2}{\mathcal{T}}\int_0^{\mathcal{T}} \frac{dt}{2i}\text{Tr}_{\text{dot}}[\mathcal{S}(-i\omega)\mathcal{F}^{\delta_{lL}+\delta_{l'L},\delta_{lR}+\delta_{l'R}}(-i\omega)$$
$$- \mathcal{S}(i\omega)\mathcal{F}^{\delta_{lL}+\delta_{l'L},\delta_{lR}+\delta_{l'R}}(i\omega)], \tag{37}$$

where the components of the superoperator $\mathcal{S}(s)$ are given by

$$[\mathcal{S}(s)]_{lmk;l'm'k'} = (s - ik\Omega)\delta_{ll'}\delta_{mm'}\delta_{kk'}. \tag{38}$$

To clarify the meaning of this definition, we note that the superoperator $\mathcal{S}(s)$ acts on an arbitrary operator A with Fourier-transformed matrix elements $A_{lm;k}$ in our standard basis $|l\rangle,|m\rangle = |0\rangle,|\uparrow\rangle,|\downarrow\rangle,|\uparrow\downarrow\rangle$ as

$$[\mathcal{S}(s)A]_{lm;k} = \sum_{l'm'}\sum_{k'}[\mathcal{S}(s)]_{lmk;l'm'k'}A_{l'm';k'}. \tag{39}$$

The derivation of the generalized MacDonald formula is outlined in the Appendix. In evaluating the current noise from the generalized MacDonald formula, we encounter the Laplace transforms $\mathcal{F}^{m,n}(s)$ of the moments of the electron-number operators in the leads. These moments are nothing but the expansion coefficients of $\mathcal{F}$ defined in Eq. (15).

Taking the trace over the dot degrees of freedom and the average over one period makes only the matrix elements $\mathcal{F}_{ll;k=0}^{m,n}$ of $\mathcal{F}^{m,n}$ that are diagonal in the dot basis and have Floquet index $k=0$ contribute to the final result. We arrive at the expression

$$\frac{\bar{S}_{ll'}(\omega)}{\omega} = -e^2\omega \, \text{Tr}_{\text{dot}}[\mathcal{F}_{k=0}^{\delta_{lL}+\delta_{l'L},\delta_{lR}+\delta_{l'R}}(-i\omega)$$
$$+ \mathcal{F}_{k=0}^{\delta_{lL}+\delta_{l'L},\delta_{lR}+\delta_{l'R}}(i\omega)]. \tag{40}$$

Now we require the charge moments in the left and right leads. They can be obtained from the equation of motion for $\mathcal{F}$ [Eq. (19)]. Suppose we switch on the counting fields at some time t_1, before that time the system can be described by the density matrix without the counting fields in the (quasi) stationary limit. Since we have assumed $t_0 \to -\infty$ above, any initial correlation have died out at time t_1.[49] We set the number of electrons having tunneled into lead l up to time t_1 to zero, $N_l(t_1,t_1)=0$. After time t_1, the system evolves under the influence of the counting fields. Then, we solve the equations for $\mathcal{F}^{m,n}(t)$ by means of Laplace transformation. For example, the solution of Eq. (23) reads

$$\mathcal{F}^{0,0}(s) = [\mathcal{S}(s) - \mathcal{L}]^{-1}\mathcal{F}^{0,0}(t_1), \tag{41}$$

where $\mathcal{F}^{0,0}(t_1)$ can be found from the stationary master equation $\mathcal{L}\mathcal{F}^{0,0}=0$ in the absence of counting fields. Analogously, we find expressions for the other expansion coefficients after the Laplace transformation as

$$\mathcal{F}^{1,0} = (\mathcal{S} - \mathcal{L})^{-1}(\mathcal{J}_{1+} - \mathcal{J}_{1-})\mathcal{F}^{0,0}, \tag{42}$$

$$\mathcal{F}^{0,1} = (\mathcal{S} - \mathcal{L})^{-1}(\mathcal{J}_{2+} - \mathcal{J}_{2-})\mathcal{F}^{0,0}, \tag{43}$$

$$\mathcal{F}^{2,0} = (\mathcal{S} - \mathcal{L})^{-1}[2(\mathcal{J}_{1+} - \mathcal{J}_{1-})\mathcal{F}^{1,0} + (\mathcal{J}_{1+} + \mathcal{J}_{1-})\mathcal{F}^{0,0}], \tag{44}$$

$$\mathcal{F}^{0,2} = (\mathcal{S} - \mathcal{L})^{-1}[2(\mathcal{J}_{2+} - \mathcal{J}_{2-})\mathcal{F}^{0,1} + (\mathcal{J}_{2+} + \mathcal{J}_{2-})\mathcal{F}^{0,0}], \tag{45}$$

$$\mathcal{F}^{1,1} = (\mathcal{S} - \mathcal{L})^{-1}[(\mathcal{J}_{1+} - \mathcal{J}_{1-})\mathcal{F}^{0,1} + (\mathcal{J}_{2+} - \mathcal{J}_{2-})\mathcal{F}^{1,0}], \tag{46}$$

where we have omitted the arguments s. The solutions for these coefficients together with the generalized MacDonald formula [Eq. (37)] give the desired time-averaged current-noise spectra of the ac-driven quantum dot. The approach presented in this study can easily be generalized to take more complex structures with multiple levels and interlevel transitions into account.

III. RESULTS AND DISCUSSION

In the following, we present our numerical results based on the Floquet master-equation method and discuss the transport properties of the single-level quantum dot with time-dependent fields. An additional dc magnetic field along the z or x direction is taken into account; it splits the energy levels of the singly charged quantum dot due to the Zeeman effect. In the present study, we choose the ac field to be either a rotating magnetic field in the xy plane or an ac gate voltage. The ac gate voltage and the rotating magnetic field will affect the quantum conductor in quite different manners. An ac gate voltage only changes the eigenvalues of $H_{\mathrm{dot}}(t)$ periodically, which in the adiabatic limit of large $\mathcal{T}$ become the eigenenergies. The ac gate voltage will not induce any transition between different eigenstates of $H_{\mathrm{dot}}(t)$ (no spin flip is possible) because the eigenstates are unaffected by the gate voltage. The electron is trapped in one spin state. The situation is different for a rotating magnetic field. A rotating magnetic field does not change the eigenvalues of $H_{\mathrm{dot}}(t)$ but does change the eigenstates and thus can flip the spin of the electron. The spin polarization of the dot will thus evolve with the rotating magnetic field. The two types of ac fields show drastically different behaviors in the transport properties as we will show below.

The full Hamiltonian of the quantum dot is written as (we reiterate that we choose $|e| = \hbar = k_B = 1$)

$$H_{\mathrm{dot}} = \sum_{\sigma} (eV_G + V_{\mathrm{ac}} \cos \Omega t + \sigma B_z) d_\sigma^\dagger d_\sigma + U d_\uparrow^\dagger d_\uparrow d_\downarrow^\dagger d_\downarrow$$
$$+ B_x (d_\uparrow^\dagger d_\downarrow + d_\downarrow^\dagger d_\uparrow) + B_{\mathrm{ac}} (d_\uparrow^\dagger d_\downarrow e^{i\Omega t} + d_\downarrow^\dagger d_\uparrow e^{-i\Omega t}), \tag{47}$$

where eV_G is the on-site energy of the quantum dot due to the dc component of the gate voltage V_G, V_{ac} is the amplitude of the oscillating gate voltage, U represents the intradot Coulomb interaction, and B_x and B_z are half the Zeeman energies of the singly occupied dot due to the dc magnetic fields in the x and z direction, respectively. Half the Zeeman energy of the rotating magnetic field is given by B_{ac}. Note that while

it is customary to talk about photon-assisted processes in this context, the treatment of the electromagnetic field in the Hamiltonian is completely classical.

We work in the sequential-tunneling regime and choose a symmetric-coupling geometry with $a = b$. We assume that the bias voltage V_{dc} symmetrically shifts the chemical potentials by $\mu_{L,R} = \pm eV_{\mathrm{dc}}/2$. In the framework of wideband approximation, the tunneling rate is given by $\Gamma_{mn;ij}^{l\sigma}(\epsilon) = 2\pi V_{l,k,\sigma}^{ij} V_{l,k,\sigma}^{mn*}$, where we have assumed the coupling strength $V_{l,k,\sigma}^{ij} = V$ to be a constant and have set the density of states of lead l to unity. In the present study, we have assumed the tunneling matrix to be independent of the energy and the occupation number on the dot. An inclusion of state-dependent tunneling is straightforward. We assume that the electrons tunneling in and out of the dot with an energy-independent rates $\Gamma = \Gamma_{mn;ij}^{l\sigma}(\epsilon)$ and set $\Gamma = 1$ as the energy unit.

A. Differential conductance

We start our discussion with the differential conductance. The gray-scale plot Fig. 1 shows the differential conductance dI/dV_{dc} vs the dc bias voltage V_{dc} and the gate voltage V_G with or without an ac field. The calculations are for the Coulomb interaction strength $U = 24$ and the temperature $k_B T = 0.32$. The frequency of the ac field is $\Omega = 8$.

Without an ac field, Fig. 1(a) gives the familiar diamond structure due to the Coulomb blockade. Numerical results for the differential conductance when the quantum dot is modulated by an ac gate voltage are presented in Fig. 1(b). Figure 1(c) gives the results when the quantum dot is modulated by a rotating magnetic field. Figure 1(d) shows the differential conductance when the quantum dot is modulated by a rotating magnetic field in the xy plane while a dc magnetic field is applied in the x direction, i.e., in the plane of the rotating magnetic field.

When there is an ac field, several striking features emerge in the differential conductance: (1) at the edge of the Coulomb diamond, the sharp differential-conductance peak for the dc transport shown in Fig. 1(a) is partially suppressed by the ac gate voltage or the rotating magnetic field. Note the different gray scales in Figs. 1(a)–1(d). This can be attributed to the suppression of the elastic resonant peak by the photon-assisted processes. (2) In the presence of an ac field, there are lines parallel to the edges of the Coulomb diamond. The distance of these lines to the peak position is approximately the frequency of the ac field, indicating a photon-assisted tunneling process. (3) An interesting feature of these lines can be observed inside the Coulomb diamonds. For the ac gate voltage, the Floquet quasienergies are spin degenerate. Therefore, the main lines in the differential-conductance plot in Fig. 1(b) are not split. However, satellites due to photon-assisted inelastic tunneling events appear in which an energy quantum of Ω is absorbed from or emitted into the driving field. We see from Fig. 1(b) that these additional lines remain distinct inside the Coulomb diamond. On the other hand, when the quantum dot is driven by a rotating magnetic field, the quasienergies are not degenerate. Therefore, the main elastic lines are split into two at the edge of the Coulomb
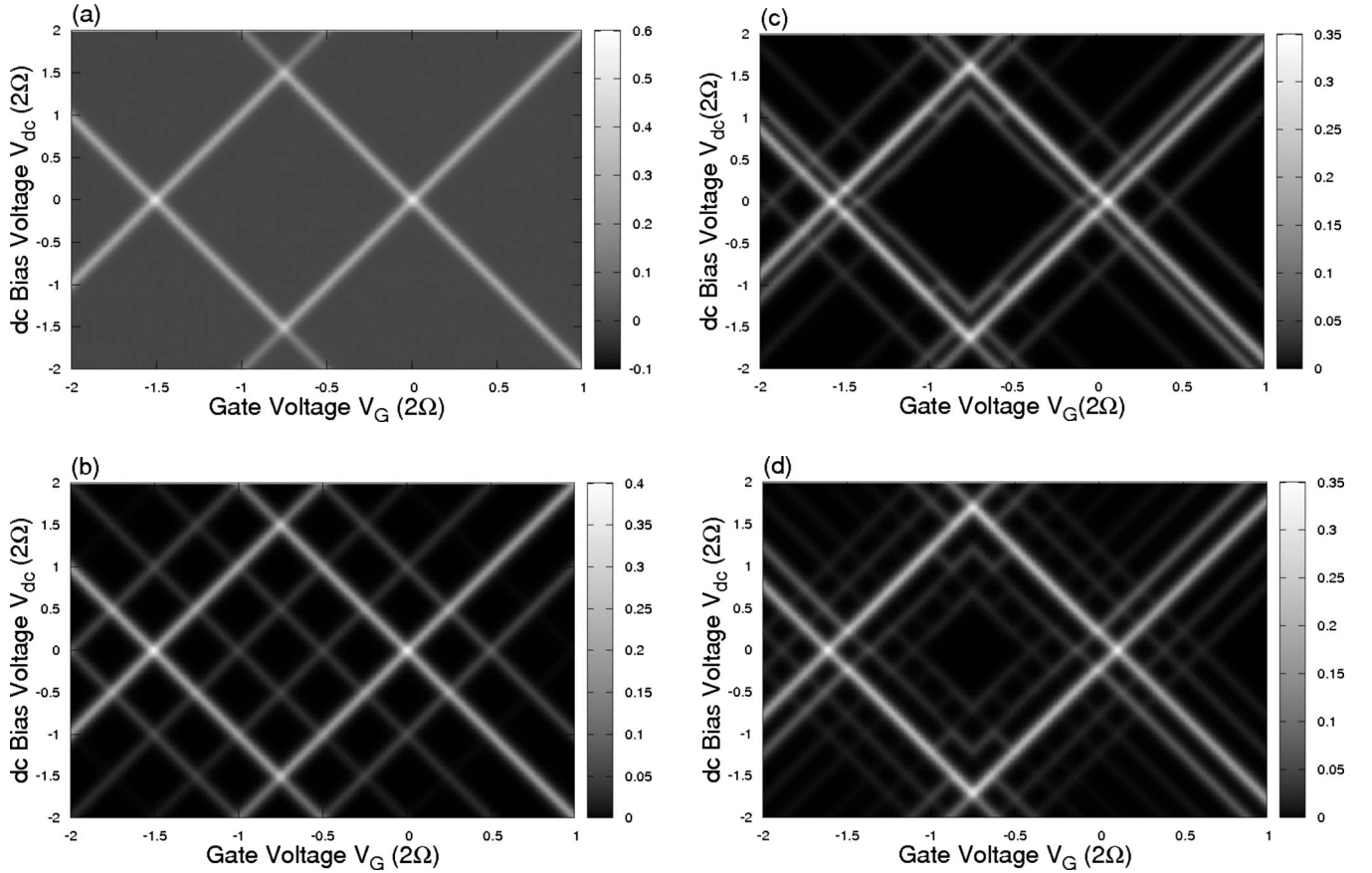
FIG. 1. Gray-scale plots of the differential conductance dI/dV_{dc} as a function of the dc bias voltage and the dc gate voltage for a quantum dot (a) without any ac fields, (b) modulated by an ac gate voltage, (c) modulated by a rotating magnetic field, and (d) modulated by a rotating magnetic field and with an additional dc magnetic field applied in the plane of the rotating field. Dark regions represent low differential conductance. The frequency of the ac field is $\Omega=8$. The amplitude of the ac gate voltage in (b) and of the rotating magnetic field in (c) and (d) are $V_{ac}=6.4$ and $B_{ac}=3.2$, respectively. The dc magnetic field in (d) is $B_x=1.6$.

diamond in Fig. 1(c). Interestingly, the lines due to the photon-assisted tunneling now only appear outside of the Coulomb diamond, as can be seen in Fig. 1(c), indicating that the photon-assisted tunneling is forbidden inside the Coulomb diamond. When the quantum dot is modulated by a rotating magnetic field and a dc magnetic field is applied in the plane of the rotating field, these lines in the Coulomb-blockade regime revive. This can be clearly seen in Fig. 1(d).

The disappearance of the photon-assisted tunneling inside the Coulomb diamond for a pure rotating magnetic field can be understood as follows. In the Coulomb diamond, the Floquet quasienergies corresponding to the singly occupied states are far below the Fermi energies of the two leads. A direct tunneling between the dot and the leads is forbidden due to the Pauli principle and Coulomb blockade. Therefore, an electron is effectively trapped in one quantum state on the dot. According to our previous discussion, only the spin direction of this quantum state can evolve with the rotating magnetic field. However, its eigenvalues of $H_{dot}(t)$ remain unchanged. Therefore, the electron cannot gain extra energy from the ac magnetic field. As a consequence, we cannot observe lines due to photon-assisted tunneling inside the Coulomb diamond. Outside of the Coulomb diamond, the tunneling between the dot and the leads becomes possible.

When an electron is injected from the lead into the dot, the system can absorb or emit photons, i.e., the Floquet index k can change. One could say that transport happens via several Floquet channels. Such photon-mediated tunneling can then give rise to the photon-assisted differential-conductance peaks.

The situation becomes different when a dc magnetic field is applied in the plane of the rotating magnetic field as shown in Fig. 1(d). In that case, the eigenstates and the eigenvalues of $H_{dot}(t)$ change periodically. Electrons can gain extra energy from the ac field by absorbing or emitting a photon. In the Coulomb diamond, electrons on the dot are able to tunnel out via the photon-assisted tunneling and we again find the lines due to the photon-assisted differential-conductance peaks inside the Coulomb diamond as shown in Fig. 1(d).

B. Zero-frequency Fano factor

In the following, we show numerical results for the time-averaged zero-frequency noise of the quantum dot. The zero-frequency noise has been studied by the quantum-master-equation method in the stationary[12,16,23] and also in the time-dependent case.[44] Without ac field and at zero temperature, the zero-frequency Fano factor $S(0)/2eI$ describes the devia-
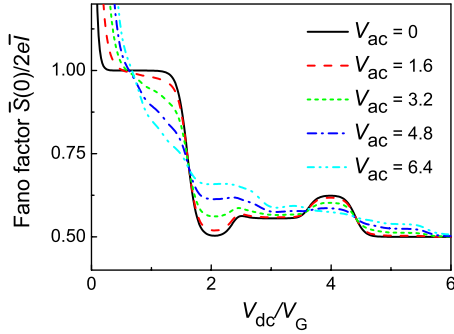
FIG. 2. (Color online) Fano factor of the quantum dot as a function of dc bias voltage V_{dc} in unit of V_G for different amplitudes V_{ac} of the ac gate voltage. The parameters of the device are given in the text.
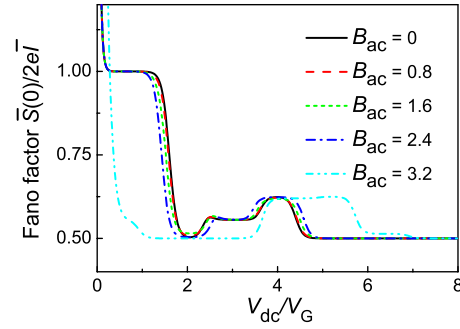

FIG. 3. (Color online) Fano factor of the quantum dot as a function of dc bias voltage V_{dc} in unit of V_G for different amplitudes B_{ac} of the rotating magnetic field. The other parameters are the same with those of Fig. 2.

tion of the shot noise from its Poissonian value. We choose the parameters $T=0.32$, $U=8$, $eV_G=8$, and $\Omega=4.8$. We assume that a dc magnetic field in the z direction, $B_z=1.6$, is applied to the quantum dot. The finite value of U and the Zeeman splitting make it possible to see plateaus in the Fano factor at different occupation numbers on the dot.[16] Figure 2 shows the zero-frequency Fano factor as a function of the dc bias with or without an ac gate voltage.

Without an ac gate voltage, $V_{ac}=0$, the results reproduce the main features reported in Ref. 16. At very low bias voltage $V_{dc} \rightarrow 0$, the main contribution to the noise is the finite thermal noise while the current as well as the shot noise are suppressed. Therefore, the Fano factor diverges at $V_{dc}=0$. For low dc bias voltage, the quantum dot operates in the Coulomb-blockade regime. With further increasing dc bias voltage, the energy levels of the quantum dot one by one enter the transport window defined by the dc bias. This can be clearly identified in the Fano factor by the plateaus at different values. The edges of the plateaus are broadened by the finite temperature. For very large dc bias, where all the energy levels of the quantum dot lie in the transport window, the Fano factor approaches the well-known limit of 1/2 for our symmetric-coupling case.[16]

The results for the dc case demonstrate that the plateaus of the Fano factor can give a good account of the transport channels.[16] In the presence of an ac field, we now consider the time-averaged Fano factor $\bar{S}(0)/2e\bar{I}$. We can see from Fig. 2 that for small V_{dc} the Fano factor becomes larger as we increase the amplitude of the ac gate voltage. On the other hand, additional photon-assisted transport channels are available due to the ac field, which will modify the Fano-factor curve. With increasing ac field, the Fano factor will thus deviate from the plateau behavior seen in dc case due to the opening of these photon-assisted transport channels. When the ac gate voltage is large enough, the Floquet eigenstates that lie outside of the transport window can contribute to the current via photon-assisted tunneling. As a consequence, the plateaus in the Fano-factor curve become vague. For very large bias voltages, all the Floquet levels are well inside the transport window. The Fano factor then will approach the same value 1/2 as for the time-independent transport. In Fig. 3, we present our results for the zero-frequency current noise in the presence of a rotating magnetic field. As in the case of

an ac gate voltage, the Fano factor deviates from the dc behavior with increasing ac field. Additional plateaus can be observed in the Fano-factor curve when we vary the dc bias voltage. Transitions between plateaus result from additional Floquet channels becoming available.

C. Frequency-dependent Fano factor

Now we present our results for the full current-noise spectra of a quantum dot under an ac field. The noise spectra have previously been studied in the stationary-transport regime. An analytical expression for the noise spectrum of a single-level quantum dot can be found in Ref. 23. Unless stated otherwise, the following calculations assume $U=24$, $V_{dc}=12.7$, $T=1.6$, $\Omega=8$, and $eV_G=-8$. We introduce the frequency-dependent Fano factor $\bar{S}(\omega)/2e\bar{I}$ to characterize the time-averaged noise power. As discussed previously, the ac gate voltage and the rotating magnetic field will modulate the quantum conductor in different ways. In the following, we show that the noise spectra are also strikingly different.

In Fig. 4, we present the results for the frequency-dependent Fano factor $\bar{S}(\omega)/2e\bar{I}$ as a function of the frequency ω for different amplitudes V_{ac}. No dc magnetic field is applied. Without an ac field ($V_{ac}=0$), the noise spectrum shows a peak at zero frequency and approaches a constant value for large ω. The peak in the noise spectrum is due to
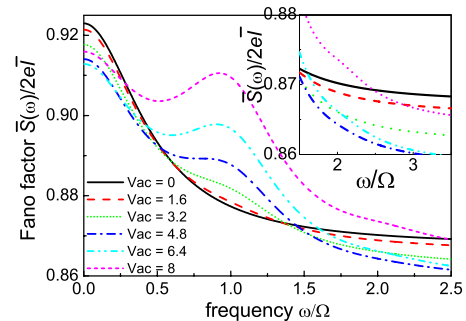

FIG. 4. (Color online) Noise spectra for different gate-voltage amplitudes V_{ac}. Independent of V_{ac}, the main peak position is fixed at Ω. The inset shows an enlarged view of the noise spectra around 2Ω.
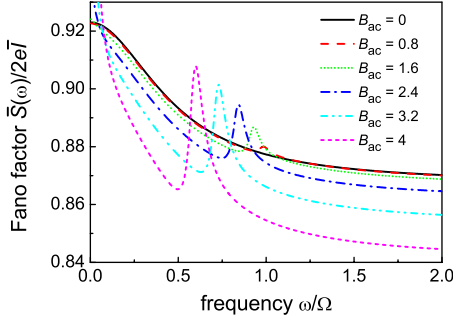
FIG. 5. (Color online) Noise spectra with a rotating magnetic field in the xy plane with various amplitudes B_{ac}. The peak position shifts with increasing B_{ac}.

the elastic processes in the transport.[29] When an ac gate voltage is applied, additional structures in the noise spectra are expected due to photon-assisted processes. For the present set of parameters, one can clearly see that with increasing amplitude of the ac gate voltage, an additional peak appears in the noise spectrum. While the height and width of this peak vary a lot with increasing amplitude, its peak position ω_p remains almost unchanged at the external driving frequency Ω.

Now we turn to the rotating magnetic field in the xy plane. In Fig. 5, we plot the Fano factor as a function of the frequency ω for different amplitudes B_{ac} of the rotating magnetic field. Similarly to the results presented in Fig. 4, a peak is generated and the width and height of this peak depend on the amplitude. However, the peak position is not fixed at Ω in contrast to what we have observed in Fig. 4 for the ac gate voltage. Instead, its position shifts with increasing amplitude, as shown in Fig. 5.

By comparing Figs. 4 and 5, we see that the peak position of the noise spectra behaves differently when we increase the ac strength, depending on the type of the ac field. Recalling that when electrons tunnel through a time-independent quantum two-level system, its current-noise spectra show additional structure at the energy difference of the two transport channels of the system due to its internal coherent dynamics,[14] we will show that the peak position of the noise spectra for ac transport can be understood from the interference between two possible Floquet transport channels. If the quantum dot is modulated by a rotating magnetic field, the last term in the dot Hamiltonian [Eq. (47)] shows that the ac magnetic field couples one spin state with the quasienergy ϵ with a state with the opposite spin and the quasienergy $\epsilon - \Omega$ (in the extended zone scheme). The coupling strength is given by B_{ac}. The corresponding Floquet Hamiltonian then decomposes into 2×2 blocks of the form

$$h_{Fl} = \begin{pmatrix} \epsilon & B_{ac} \\ B_{ac} & \epsilon - \Omega \end{pmatrix}. \tag{48}$$

The resulting quasienergies in the first Brillouin zone $[0, \Omega)$ are

$$\epsilon_1 = \epsilon - \frac{\Omega}{2} + \frac{\sqrt{\Omega^2 + 4B_{ac}^2}}{2}, \tag{49}$$

$$\epsilon_2 = \epsilon + \frac{3\Omega}{2} - \frac{\sqrt{\Omega^2 + 4B_{ac}^2}}{2} \tag{50}$$

with the difference

$$\omega_p = \epsilon_2 - \epsilon_1 = 2\Omega - \sqrt{\Omega^2 + 4B_{ac}^2} \tag{51}$$

(these expressions hold if $B_{ac} < \sqrt{3}\Omega/2$).

If now an electron tunnels into the dot, the system ends up in a superposition of the two Floquet states, the phases of which change with different angular frequencies, corresponding to spin precession with the difference frequency ω_p. When the electron tunnels out again, the superposition is projected onto the spin direction of the original electron since lead electron creation and annihilation operators are paired with identical quantum numbers in the master equation. This leads to interference with a typical frequency ω_p, which enhances the current-current correlation function $S_{ij}(t, t')$ in Eq. (30) for $t - t'$ being a multiple of the period $2\pi/\omega_p$ and thus leads to a peak in the noise spectrum at ω_p. The peaks seen in Fig. 5 are indeed centered at ω_p given by Eq. (51).

Comparing with the stationary transport through a stationary two-level system,[14] the transport through a quantum dot with rotating magnetic field can be understood as another type of two-level quantum system. The significant difference here is that our two levels are defined by the Floquet channels due to a periodic ac field and not by the true eigenenergies of an time-independent Hamiltonian.

When an ac gate voltage is applied to the quantum dot, the ac field will not couple the different spin states. Only the eigenvalues of $H_{dot}(t)$ will be modulated, see Eq. (47). The corresponding Floquet Hamiltonian decomposes into two infinite blocks for the two spin directions, where each block has the tridiagonal form

$$h_{Fl} = \begin{pmatrix} \ddots & & & \\ & \epsilon + \Omega & V_{ac}/2 & 0 \\ & V_{ac}/2 & \epsilon & V_{ac}/2 \\ & 0 & V_{ac}/2 & \epsilon - \Omega \\ & & & \ddots \end{pmatrix}. \tag{52}$$

Therefore, the electrons can tunnel through the quantum dot via infinitely many Floquet channels with the same quasienergy in the first Brillouin zone $[0, \Omega)$ but all possible Floquet indices k. The quasienergies in the extended zone scheme thus differ by integer multiples of Ω. These quasienergy differences define the peak positions in the noise spectra. In Fig. 4, a peak at Ω appears, corresponding to two channels with their Floquet indices (photon numbers) differing by unity. One should also expect peak structures at $n\Omega$, $n > 1$. However, to observe these peak structures, one may need a stronger ac field to enable multiphoton-assisted transport. In the inset of Fig. 4, a small shoulder emerges at 2Ω for the largest amplitude, $V_{ac} = 8$.

So far in our discussion, no dc magnetic field has been considered. For the quantum dot with an ac gate voltage and a dc magnetic field in the z direction, our results of the noise spectra for different voltage amplitudes are displayed in Fig.
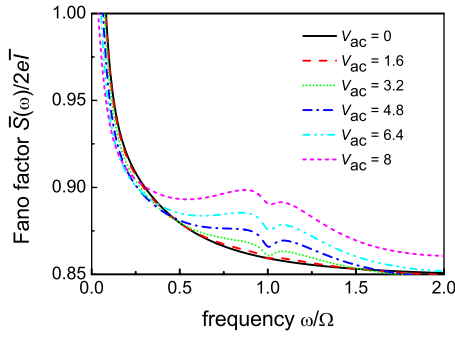
FIG. 6. (Color online) Noise spectra for a quantum dot modulated by an oscillating gate voltage with various amplitudes V_{ac} in the presence of a dc magnetic field $B_z=1.6$ in the z direction. The dip position is fixed at the driving frequency.

6. The parameters are the same as those used in Fig. 4 except that the strength of the dc magnetic field in the z direction is $B_z=1.6$. For the present set of parameters, the peak at Ω is replaced by a dip. We observe that the appearance of the peak or the dip depends on the detailed parameters used in our calculation. The peak or dip position remains unchanged as we increase the voltage amplitude. We have checked that the noise spectrum does not depend on the direction of the dc magnetic field. This is because the full SU(2) symmetry is preserved since we have included the time evolution of the off-diagonal elements of the reduced density matrix within our quantum-master-equation approach.

Contrary to the quantum dot with an ac gate voltage, for the case of a rotating magnetic field, the noise spectra do depend on the direction of the additional dc magnetic field. When the dc magnetic field is perpendicular to the plane of the rotating magnetic field, the noise spectra behave much like those for a pure rotating magnetic field. Only one peak appears at a nonzero frequency and the peak position shifts with the amplitude of the rotating magnetic field. Numerical results for the noise with a rotating magnetic in the xy plane and a dc magnetic field in the z direction are displayed in Fig. 7. The parameters are the same as in Fig. 5 and the dc magnetic field is $B_z=1.6$. It is easy to verify that the peak position can again be determined by the difference between two Floquet quasienergies.

When a nonzero dc magnetic field B_x is applied in the plane of the rotating magnetic field, the Floquet Hamiltonian
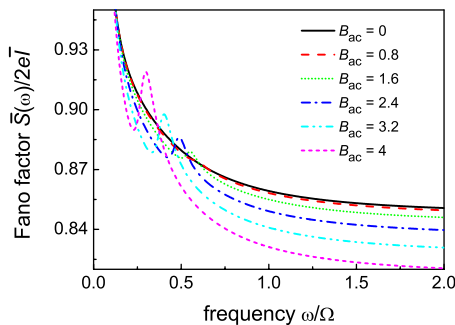

FIG. 7. (Color online) Noise spectra in the presence of a rotating magnetic field in the xy plane with various amplitudes B_{ac}. A dc magnetic field $B_z=1.6$ is applied in the z direction. Only one peak appears, which shifts with B_{ac}.
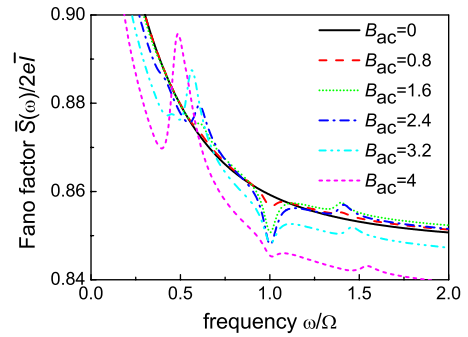

FIG. 8. (Color online) Noise spectra with a rotating magnetic field in the xy plane with various amplitudes B_{ac}. A dc magnetic field $B_x=1.6$ is applied in the x direction. New features appear in the noise spectra since more Floquet channels are involved in the transport in the presence of an in-plane magnetic field.

cannot be reduced to a 2×2 matrix form as for the previously discussed situation of vanishing dc magnetic field since the B_x term in Eq. (47) mixes spin-up and spin-down states. Together with the rotating magnetic field this couples all Floquet states with the same quasienergy in the first Brillouin zone and different Floquet indices. Thus the electrons can tunnel through the quantum dot via infinitely many Floquet channels. The interference between these Floquet channels then gives rise to much richer behavior in the noise spectra. Numerical results for the noise spectra of a quantum dot driven by a rotating magnetic field in the xy plane and with a dc magnetic field in the x direction are presented in Fig. 8. The parameters used in the calculation are the same as in Fig. 5 and the dc magnetic field in $B_x=1.6$. In Fig. 8, more peaks are observed than for vanishing dc magnetic field in Fig. 5. One can see that besides the peak determined by Eq. (51), there are both peaks (dips) fixed at Ω and structures at positions depending on the ac-field amplitude B_{ac}. All peak (dip) positions correspond to the differences of available Floquet quasienergies.

IV. SUMMARY

In this paper, the transport properties of a single-level quantum dot modulated by either an ac gate voltage or a rotating magnetic field have been studied within the Floquet quantum-master-equation approach in the sequential-tunneling limit. We have employed a generalized MacDonald formula to obtain the time-averaged current-noise spectra for both cases. Numerical results for the differential conductance and the frequency-dependent current noise have been presented. Besides the usual diamond structure due to the Coulomb blockade in the differential conductance, photon-assisted tunneling can give rise to additional lines parallel to the edges of the Coulomb diamond. These lines cannot survive inside the Coulomb diamond in the case of a rotating magnetic field. This is due to the fact that the rotating magnetic field only periodically rotates the spin direction while the energy of the electron on the dot remains unchanged. The frequency-dependent noise spectra of the quantum dot show additional peaks or dips in the presence of an ac field. The

behavior of these additional structures depends on the nature of the ac-driving field. In the case of an ac gate voltage, the position of the finite-frequency peak is fixed at the external ac frequency, independently of the voltage amplitude. On the other hand, in the case of a rotating magnetic field, the peak at nonzero frequency moves with changing amplitude of the rotating magnetic field. An additional dc magnetic field in the plane of the rotating magnetic field can also drastically change the noise spectra; it leads to the appearance of both movable and fixed peak structures in the noise spectra. All these peak positions are found to be determined by the energy differences between two Floquet transport channels.

APPENDIX: DERIVATION OF THE GENERALIZED MACDONALD FORMULA WITH ac FIELD

A derivation of the MacDonald formula for time-independent transport has been presented in Ref. 24. We show here that the periodicity of our time-dependent Hamiltonian makes it possible to estimate the noise spectra by generalizing the MacDonald formula. The derivation of the generalized MacDonald formula for the time-averaged noise spectra is outlined in the following.

We start from the Fourier-transformed current correlation function,

$$S(t,\omega) = \int_{-\infty}^{\infty} d\tau e^{i\omega\tau} \langle \{\delta I(t), \delta I(t-\tau)\} \rangle, \quad (A1)$$

where $\delta I(t) = I(t) - \langle I(t) \rangle$ and $\{A,B\} = AB + BA$. For simplicity, we omit the lead index in the noise expressions in this appendix.

From the definition of the current, we have

$$\int_{t}^{t+\tau} dt' \, \delta I(t') = \int_{t}^{t+\tau} dt' [I(t') - \langle I(t') \rangle]$$

$$= eN(t+\tau,t) - \int_{t}^{t+\tau} dt' \langle I(t') \rangle, \quad (A2)$$

where $N(t+\tau,t)$ denotes the number of charges transferred during the interval from t to $t+\tau$. Taking the expectation value of the square of this equation, we obtain

$$2e^2 \left\langle \left[N(t+\tau,t) - \int_{t}^{t+\tau} dt' \langle I(t') \rangle /e \right]^2 \right\rangle$$

$$= \left\langle \int_{t}^{t+\tau} dt' \int_{t}^{t+\tau} dt'' [\delta I(t')\delta I(t'')\delta I(t'')\delta I(t')] \right\rangle$$

$$= \int_{t}^{t+\tau} dt' \int_{t}^{t+\tau} dt'' \int_{-\infty}^{\infty} d\omega \frac{1}{2\pi} S(t',\omega) e^{i\omega(t'-t'')}. \quad (A3)$$

Inserting the Fourier decomposition of the time-dependent relation

$$S(t',\omega) = S_0(\omega) + \sum_{k\neq 0} e^{-ik\Omega t'} S_k(\omega) \quad (A4)$$

into Eq. (A3), we obtain

$$\ldots = \int_{t}^{t+\tau} dt' \int_{-\infty}^{\infty} d\omega \frac{1}{2\pi} \left[S_0(\omega) + \sum_{k}' e^{-ik\Omega t'} S_k(\omega) \right] e^{-i\omega t'} \left[\frac{1}{i\omega} (e^{i\omega(t+\tau)} - e^{i\omega t}) \right]$$

$$= \int_{-\infty}^{\infty} d\omega \frac{1}{2\pi} S_0(\omega) \frac{1}{\omega^2} (e^{-i\omega\tau} - 1)(e^{i\omega\tau} - 1) + \int_{-\infty}^{\infty} d\omega \sum_{k}' \frac{1}{2\pi} S_k(\omega) \frac{1}{\omega(\omega+k\Omega)} e^{-ik\Omega t} (e^{-i(\omega+k\Omega)\tau} - 1)(e^{i\omega\tau} - 1),$$

$$= \int_{-\infty}^{\infty} d\omega \frac{1}{\pi} S_0(\omega) \frac{1}{\omega^2} [1 - \cos(\omega\pi)] + \int_{-\infty}^{\infty} d\omega \sum_{k}' \frac{1}{2\pi} S_k(\omega) \frac{e^{-ik\Omega t}}{\omega(\omega+k\Omega)} [e^{-ik\Omega\tau} - e^{-i(\omega+k\Omega)\tau} - e^{i\omega\tau} + 1], \quad (A5)$$

where we have used the notation $\sum_{k}' = \sum_{k\neq 0}$. Differentiation with respect to τ gives

$$\frac{d}{d\tau} 2e^2 \left\langle \left[N(t+\tau,t) - \int_{t}^{t+\tau} dt' \langle I(t') \rangle /e \right]^2 \right\rangle = \int_{-\infty}^{\infty} d\omega \frac{1}{\pi} \frac{S_0(\omega)}{\omega} \sin\omega\tau + \int_{-\infty}^{\infty} d\omega \sum_{k}' \frac{1}{2\pi} S_k(\omega) e^{-ik\Omega t} \frac{1}{\omega(\omega+k\Omega)} (-ik\Omega e^{-ik\Omega\tau}$$

$$+ i(\omega+k\Omega) e^{-i(\omega+k\Omega)\tau} - i\omega e^{i\omega\tau}). \quad (A6)$$

We next perform a Fourier transformation and take the time average over one period. The second term on the right-hand side vanishes due to its periodicity. Since the current correlation function is symmetric, $S(t,t') = S(t',t)$, it can be shown that $\bar{S}(\omega) = \frac{1}{T} \int_0^T dt \int_{-\infty}^{\infty} dt' S(t,t') e^{i\omega(t-t')}$ has the property $\bar{S}(\omega) = \bar{S}(-\omega)$. We arrive at the generalized formula for the time-averaged noise spectrum for a periodic driving field,

$$\frac{1}{\mathcal{T}}\int_0^{\mathcal{T}} dt\, 2e^2 \int_{-\infty}^{\infty} d\tau\, e^{i\omega\tau} \frac{\partial}{\partial \tau} \left\langle \left[N(t+\tau,t) - \int_t^{t+\tau} dt' \langle I(t') \rangle / e \right]^2 \right\rangle$$

$$= \frac{1}{\mathcal{T}}\int_0^{\mathcal{T}} dt\, 2e^2 \int_{-\infty}^{\infty} d\tau\, \sin(\omega\tau) \frac{\partial}{\partial \tau} \left\langle \left[N(t+\tau,t) \right. \right.$$

$$\left. \left. - \int_t^{t+\tau} dt' \langle I(t') \rangle / e \right]^2 \right\rangle = 2i \frac{\bar{S}(\omega)}{\omega}. \tag{A7}$$

Noting that the integrand of the τ integral is even, we obtain the final result for the generalized MacDonald formula for the time-averaged noise spectrum,

$$\frac{\bar{S}(\omega)}{\omega} = 2e^2 \frac{1}{\mathcal{T}}\int_0^{\mathcal{T}} dt \int_0^{\infty} d\tau\, \sin \omega\tau \frac{\partial}{\partial \tau} \left\langle \left[N(t+\tau,t) \right. \right.$$

$$\left. \left. - \int_t^{t+\tau} dt' \langle I(t') \rangle / e \right]^2 \right\rangle. \tag{A8}$$

In comparison to the MacDonald formula for steady-state transport, an integration of t over one period is carried out to obtain the time-averaged noise spectra. The time average can also be expressed by an average over the initial phase of the ac field. Hence, our expression is equivalent to the form given by Clerk and Girvin.[46]

*bhwu@mail.sim.ac.cn

†carsten.timm@tu-dresden.de

[1] J. R. Heath and M. A. Ratner, Phys. Today **56**(5), 43 (2003).

[2] L. S. Levitov, H. W. Lee, and G. B. Lesovik, J. Math. Phys. **37**, 4845 (1996).

[3] C. Flindt, T. Novotny, and A.-P. Jauho, Phys. Rev. B **70**, 205334 (2004).

[4] M. Vanevic, Y. V. Nazarov, and W. Belzig, Phys. Rev. Lett. **99**, 076601 (2007).

[5] *Quantum Noise in Mesoscopic Physics*, edited by Y. V. Nazarov (Kluwer Academic, Dordrecht, 2003).

[6] J. Koch and F. von Oppen, Phys. Rev. Lett. **94**, 206804 (2005).

[7] J. Koch, F. von Oppen, and A. V. Andreev, Phys. Rev. B **74**, 205438 (2006).

[8] X. Zhong and J. C. Cao, J. Phys.: Condens. Matter **21**, 295602 (2009).

[9] J. Bylander, T. Duty, and P. Delsing, Nature (London) **434**, 361 (2005).

[10] T. Fujisawa, T. Hayashi, R. Tomita, and Y. Hirayama, Science **312**, 1634 (2006).

[11] S. Gustavsson, R. Leturcq, B. Simovič, R. Schleser, T. Ihn, P. Studerus, K. Ensslin, D. C. Driscoll, and A. C. Gossard, Phys. Rev. Lett. **96**, 076605 (2006).

[12] Y. M. Blanter and M. Büttiker, Phys. Rep. **336**, 1 (2000).

[13] O. Zarchin, M. Zaffalon, M. Heiblum, D. Mahalu, and V. Umansky, Phys. Rev. B **77**, 241303(R) (2008).

[14] R. Aguado and T. Brandes, Phys. Rev. Lett. **92**, 206601 (2004).

[15] F. W. J. Hekking and J. P. Pekola, Phys. Rev. Lett. **96**, 056603 (2006).

[16] A. Thielmann, M. H. Hettler, J. König, and G. Schön, Phys. Rev. B **68**, 115105 (2003).

[17] E. A. Rothstein, O. Entin-Wohlman, and A. Aharony, Phys. Rev. B **79**, 075307 (2009).

[18] S. Camalet, J. Lehmann, S. Kohler, and P. Hänggi, Phys. Rev. Lett. **90**, 210602 (2003).

[19] B. H. Wu and J. C. Cao, Phys. Rev. B **77**, 233307 (2008).

[20] B. H. Wu and J. C. Cao, arXiv:0906.5266, Phys. Rev. B (to be published).

[21] M. Braun, J. König, and J. Martinek, Phys. Rev. B **74**, 075328 (2006).

[22] D. K. C. MacDonald, Rep. Prog. Phys. **12**, 56 (1948).

[23] J. Y. Luo, X. Q. Li, and Y. J. Yan, Phys. Rev. B **76**, 085325 (2007).

[24] N. Lambert, R. Aguado, and T. Brandes, Phys. Rev. B **75**, 045340 (2007).

[25] B. Dong, X. L. Lei, and N. J. M. Horing, J. Appl. Phys. **104**, 033532 (2008).

[26] P. K. Tien and J. P. Gordon, Phys. Rev. **129**, 647 (1963).

[27] P. W. Brouwer, Phys. Rev. B **58**, R10135 (1998).

[28] S. D. Barrett and T. M. Stace, Phys. Rev. Lett. **96**, 017405 (2006).

[29] J. Wabnig, B. W. Lovett, G. A. D. Briggs, and J. H. Jefferson, Phys. Rev. Lett. **102**, 016802 (2009).

[30] G. Floquet, Ann. Sci. Ec. Normale Super. **12**, 47 (1883).

[31] M. Grifoni and P. Hänggi, Phys. Rep. **304**, 229 (1998).

[32] M. Moskalets and M. Büttiker, Phys. Rev. B **66**, 205320 (2002).

[33] B. H. Wu and J. C. Cao, Phys. Rev. B **73**, 245412 (2006).

[34] V. Gudmundsson, G. Thorgilsson, C. S. Tang, and V. Moldoveanu, Phys. Rev. B **77**, 035329 (2008).

[35] L. E. F. Foa Torres, Phys. Rev. B **72**, 245339 (2005).

[36] L. Arrachea, Phys. Rev. B **72**, 125349 (2005).

[37] B. H. Wu and J. C. Cao, J. Phys.: Condens. Matter **20**, 085224 (2008).

[38] H.-P. Breuer and F. Petruccione, *The Theory of Open Quantum Systems* (Oxford University Press, Oxford, 2002).

[39] C. Timm, Phys. Rev. B **77**, 195416 (2008).

[40] F. Elste and C. Timm, Phys. Rev. B **71**, 155403 (2005).

[41] R. Blümel, A. Buchleitner, R. Graham, L. Sirko, U. Smilansky, and H. Walther, Phys. Rev. A **44**, 4521 (1991).

[42] H.-P. Breuer, W. Huber, and F. Petruccione, Phys. Rev. E **61**, 4883 (2000).

[43] J. Lehmann, S. Kohler, V. May, and P. Hänggi, J. Chem. Phys. **121**, 2278 (2004).

[44] F. J. Kaiser and S. Kohler, Ann. Phys. (Leipzig) **16**, 702 (2007).

[45] F. Cavaliere, M. Governale, and J. König, Phys. Rev. Lett. **103**, 136801 (2009).

[46] A. A. Clerk and S. M. Girvin, Phys. Rev. B **70**, 121303(R) (2004).

[47] S. Datta, arXiv:cond-mat/0603034 (unpublished).

[48] M. Esposito and M. Galperin, Phys. Rev. B **79**, 205303 (2009).

[49] C. Flindt, T. Novotny, A. Braggio, M. Sassetti, and A.-P. Jauho, Phys. Rev. Lett. **100**, 150601 (2008).

[50] S. Ramo, Proc. IRE **27**, 584 (1939).

[51] W. Shockley, J. Appl. Phys. **9**, 635 (1938).

[52] H. J. Carmichael, *Statistical Methods in Quantum Optics 1: Master Equations and Fokker-Planck Equations* (Springer, Berlin, 2002).

[53] C. W. Gardiner and P. Zoller, *Quantum Noise*, 2nd ed. (Springer, Berlin, 2000).